Carbohydrate Polymers 117 (2015) 731–738

Contents lists available at ScienceDirect

Carbohydrate Polymers

journal homepage: www.elsevier.com/locate/carbpol

A method for top down preparation of chitosan nanoparticles and nanofibers

Ruchira N. Wijesena [a], Nadeeka Tissera [a], Yasun Y. Kannangara [a], Yuan Lin [b], Gehan A.J. Amaratunga [a], K.M. Nalin de Silva [a,*]

[a] Sri Lanka Institute of Nanotechnology, Nanotechnology & Science Park, Mahenwatta, Pitipana, Homagama, Sri Lanka
[b] State Key Laboratory of Polymer Physics and Chemistry, Changchun Institute of Applied Chemistry, Chinese Academy of Sciences, Changchun 130022, PR China

ARTICLE INFO

Article history:
Received 18 July 2014
Received in revised form 16 October 2014
Accepted 17 October 2014
Available online 30 October 2014

Keywords:
Chitosan nanoparticles
Chitosan nanofibers
Top down
Chitin nanofibers
Ultrasonication

ABSTRACT

A method of top down preparation of chitosan nanoparticles and nanofibers is proposed. Chitin nanofibrils (chitin NFs) were prepared using ultrasonic assisted method from crab shells with an average diameter of 5 nm and the length less than 3 μm as analyzed by atomic force microscopy and transmission electron microscopy. These chitin nanofibers were used as the precursor material for the preparation of chitosan nanoparticles and nanofibers. The degree of deacetylation of these prepared chitosan nanostructures were found to be approximately 98%. In addition these chitosan nanostructures showed amorphous crystallinity. Transmission electron microscopic studies revealed that chitosan nanoparticles were roughly spherical in nature and had diameters less than 300 nm. These larger particles formed through self-assembly of much smaller 25 nm particles as evidenced by the TEM imaging. The diameter and the length of the chitosan nanofibers were found to be less than 100 nm and 3 μm respectively. It is envisaged that due to the cavitation effect, the deacetylated chitin nanofibers were broken down to small pieces to form seed particles. These seed particles can then be self-assembled to form larger chitosan nanoparticles.

1. Introduction

Chitosan, the cationic (1-4)-2-amino-2-deoxy-β-D-glucan partly acetylated to the typical extent close to 0.20, is industrially produced from marine chitin, the linear (1-4)-2-acetamido-2-deoxy-β-D-glucan. Both of them have attracted attention owing to their superior characteristic properties, among which biocompatibility and absence of toxicity (Baxter, Dillon, Anthony Taylor, & Roberts, 1992).

Chitosan based nanostructures are an area of active research due to their potential applications in many different fields (Elsabee, Naguib, & Morsi, 2012; Fuente et al., 2010; Garcia-Fuentes & Alonso, 2012; Jayakumar, Prabaharan, Sudheesh Kumar, Nair, & Tamura, 2011; Muzzarelli, 2012). Nanoparticles and nanofibers are of particular importance due to their potential applications in biomedical and drug delivery systems (Elsabee et al., 2012; Muzzarelli, 2011; Shukla, Mishra, Arotiba, & Mamba, 2013).

Electrospinning has emerged as the most popular method of preparation of chitosan nanofibers due to relative ease and flexibility it offers (Jayakumar, Prabaharan, Nair, & Tamura, 2010). However fabrication of nanofibers having diameters less than 50 nm remains a challenge in electrospinning (Jayakumar et al., 2010). A different strategy for bottom up preparation of chitin nanofibers was presented by Chao and co-workers where fibers are self assembled on a surface through drying of a polymer solution (Zhong et al., 2010).

In contrast to nanofibers, chitosan nanoparticles can be prepared using a number of different strategies. These include emulsification and cross linking, ionotropic gelation, microemulsion, emulsification solvent diffusion, polyelectrolyte complexation and desolvation (Grenha, 2012). All these techniques adopt a "bottom-up" approach where nanoparticles are generated from individual macromolecules through self-assembly (Iqbal, Preece, & Mendes, 2012). Although different methods have their merits, toxicity of crosslinking and complexation agents used in some of them may limit their suitability in applications (Andersen, Hägerstrand, & Nordberg, 1982; Zeiger, Gollapudi, & Spencer, 2005).

"Top-down" approach in nanofabrication refers to the creation of a nanostructure from a larger parent superstructure through disintegration (Iqbal et al., 2012). When the extent of work

* Corresponding author. Tel.: +94 714406276; fax: +94 114741995.
E-mail addresses: kmnd@chem.cmb.ac.lk, nalinds@slintec.lk (K.M.N. de Silva).

http://dx.doi.org/10.1016/j.carbpol.2014.10.055
0144-8617/

carried out by adopting bottom-up strategies to prepare chitosan nanostructures is compared, research carried out using top down technologies is almost insignificant. There are only few reports on the preparation of chitosan nanofibers/nano-whiskers through disassembly of chitosan flakes (Liu, Chang, Chen, & Wu, 2011; Liu, Wu, Chang, & Gao, 2011; Zhou & Wu, 2011). Both these research groups have reported almost identical strategy for preparation of chitosan nanofibers, which is based on wet grinding followed by high pressure homogenization. Both groups have reported that the diameter of the nanofiber to be in the range of 100–1000 nm and the length of the fiber to be higher than 1 μm.

Herein, we report a strategy for top-down preparation of chitosan nanofibers and nanoparticles starting from chitin flakes as the precursor material. These nanostructures were prepared through a chitin nanofiber pathway as opposed to the previous work that utilizes chitosan flakes as the initial source. Further, we have used ultrasonication as the technique for mechanical disassembly. The objective of this work is to investigate the properties of chitosan nanofibers and nanoparticles prepared using above mentioned strategy.

2. Experimental methods

2.1. Materials

Raw crab shells (*Portunus pelagicus*) were thoroughly washed and separated according to their size. Crab shells having carapace length of only 14 ± 1 cm was selected for the experiments since this length usually corresponds to the fully grown species. Reagent grade sodium hydroxide, hydrochloric acid, sodium acetate, Hydrogen peroxide and acetic acid were obtained from Sigma Aldrich (USA). Chitosan flakes were obtained from HiMedia laboratories (India) having a purity level of 99% and degree of deacetylation higher than 85%. Distilled water was used in all the experiments.

2.2. Methods

2.2.1. Sample preparation for chitin extraction

Crab shells were thoroughly washed to remove any soluble organics and adhering impurities including soil and protein. Cleaned samples were completely dried in an oven at 60 °C for 24 h. Dried shells were grounded using porcelain mortar and pestle. For the purpose of obtaining uniform size crab shell powder, grounded crab shell was sifted through 1 mm and 0.75 mm sieves (Impact Test Sieve, Impact Test Equipments Ltd., UK). Several fractions of samples were kept inside a desiccator until future use.

2.2.2. Preparation of chitin nanofibers

Modified version of already well-established method for chitin nanofiber preparation was adopted in this research (Fan, Fukuzumi, Saito, & Isogai, 2012; Fan, Saito, & Isogai, 2008, 2010; Ifuku et al., 2011). Crab shell powder was dispersed in a 1 M sodium hydroxide solution at 80 °C for 10 h under vigorous stirring. Once completed the reaction mixture was cooled down to room temperature, and washed with distilled water using three sediment-decant cycles. Precipitate obtained from the above procedure was treated with 2.5 M HCl solution for removal of $CaCO_3$ from the crab shell. The reaction was carried out for 2 days at room temperature with continuous stirring. Once completed, precipitate was washed with distilled water using three sediment-decant cycles. After washing, sample was again charged with 1 M sodium hydroxide solution and stirred for 2 days at room temperature to remove residual proteins completely. Then the pigmented compounds were bleached using 3% (v/v) solution of H_2O_2 maintained at pH of 10.5 ± 0.5 using sodium acetate, reacting for 20 min at 80 °C.

Ultrasound was used to facilitate the fibrillation of prepared chitin flakes using an ultrasound tip sonicator operating at frequency of 24 kHz and 360 W power (UP400S, Hielscher Ultrasound Technology, Germany). Initially, the sample was dispersed in water at 1% (w/v) concentration. The pH was set to 3–4 using acetic acid which helps to increase the repulsive forces between chitin nanofibers thus enhancing the dispersibility (Fan et al., 2008; Ifuku et al., 2009). Then the sample was transferred to a glass beaker (250 ml) and sonicated for 2 h. Finally a semitransparent solution with slight bluish color was obtained which is characteristic for chitin nanofiber dispersion. The dispersion was stable for days at current pH.

2.2.3. Deacetylation of chitin nanofibers

Deacetylation of chitin was achieved by treating chitin nanofiber dispersion with 50% (w/v) concentrated solution of NaOH. Reaction was carried out inside a conical flask with constant stirring at 120 °C for 30 min. Once completed, excess solution was drained and the remaining product was washed using several sediment-decant cycles with excess water until solution is neutral to litmus. The resulted dispersion was bluish color indicating light scattering from small particles. Unlike the chitin NFs dispersion, the stability of resulted dispersion was poor at neutral pH and produced cloudy agglomerations followed by precipitation within minutes after dispersing. From here on deacetylated chitin NFs will be referred to as D-chitin NFs.

2.2.4. Preparation of chitosan nanofibers and nanoparticles

Chitosan nanofibers and nanoparticles were prepared using direct ultrasonication of D-chitin NFs dispersion. Before sonication, concentration of the dispersion was adjusted to 0.1% (w/v) in a 100 ml glass beaker. Ultrasonication was carried out using ultrasound tip operating at 24 kHz frequency and 360 W power (UP400S, Hielscher Ultrasound Technology, Germany) for 15 min. Centrifugation technique was utilized for separation of chitosan nanoparticles (chitosan NPs) and chitosan nanofibers (chitosan NFs) from water soluble chitosan oligomers. Before centrifugation, the solution was diluted in 9 fold in distilled water. Then the solution was centrifuged at 9000 rpm to separate water soluble chitosan oligomers. Separation of chitosan NPs and chitosan NFs was difficult with centrifugation technique as resulting dispersion is not stable. However, chitosan NPs could be separated using simple gravity filtration using ash-less cellulose filter papers (Whatman 42). Filtrate contained chitosan NPs which are almost free of chitosan NFs. Residue consisted of mostly chitosan NFs and some chitosan NPs.

3. Characterization

Morphological characterizations of chitin NFs, chitosan NPs, chitosan NFs and water soluble chitosan oligomers were performed using Atomic Force Microscope (AFM) using a Park Systems, XE-100 microscope. Imaging was carried out using non-contact mode cantilever, having a tip radius less than 10 nm operating at a scanning frequency of 0.5 Hz. Chitin NFs was first dispersed in water using ultrasound tip. Then drop of the solution was casted onto a mica piece which is later mounted on the scanning stage of AFM after complete drying.

Transmission electron microscopy (TEM) was used to characterize the morphology of the prepared samples using JEOL JEM-1011 operating at an accelerating voltage of 100 kV. Water dispersions of the nanomaterials were casted on TEM grids and allowed for drying. Dried grids were taken for inspection.

Fourier transform infrared spectroscopy (FTIR) measurements were taken for chitin flakes, chitin NFs and for the mixture of chitosan NFs and chitosan NPs (Bruker FT-IR Vertex 80). Dried samples were placed on top of the ZnSe crystal inside the ATR chamber. The

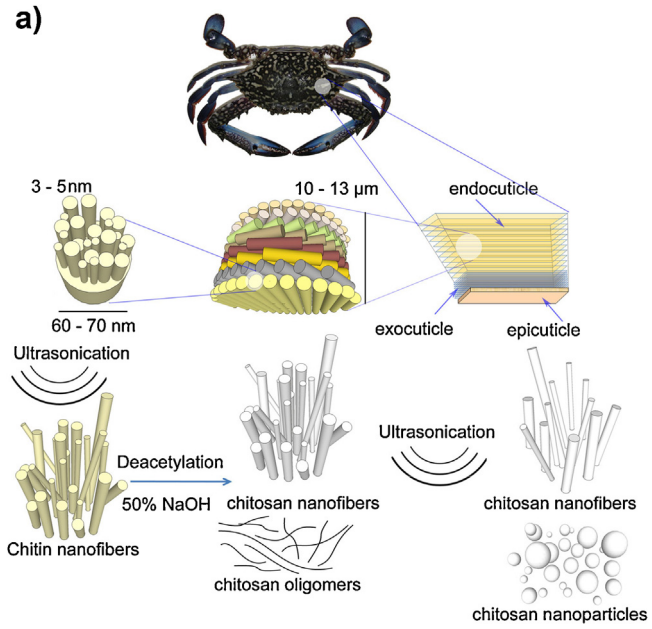

Fig. 1. (a) Process of preparation of chitosan nanofibers and chitosan nanoparticles and (b) water suspensions of chitin nanofibers (left) chitosan nanofiber/nanoparticle mixture (middle) chitosan oligomers (right).

special tightening unit that comes with the instrument was used to ensure the maximum contact between crystal and the sample. FTIR spectra were recorded between 4000 cm^{-1} and 600 cm^{-1} with the resolution of 4 cm^{-1} in the absorbance mode for 128 scans at room temperature.

X-ray diffraction (XRD) measurements were carried out using (Brucker D8 Focus X-ray Diffractometer) Cu-Kα radiation emitted from X-ray tube operated at 30 kV and 25 mA. Samples were dried for 2 h at 60 °C for removal of any excess moisture and diffraction patterns were recorded at room temperature.

Thermogravimetric analysis (TGA) was performed for finely grounded chitin flakes, chitosan flakes, chitin NFs and chitosan NFs and chitosan NPs mixture using Q-600 TGA from TA-Instruments. Approximately 9–10 mg of the sample was placed inside the alumina pan and heated from 30 °C to 700 °C at a heating rate of 20 °C/min under a N_2 purge of 100 ml/min.

4. Results and discussion

4.1. Preparation of chitosan NPs and chitosan NFs

Preparation steps of chitosan NPs and chitosan NFs starting from crab shells is schematically presented in Fig. 1(a). Crab shell is identified as a composite structure having three separate layers. Top most layer is called as epicuticle which is a nonchitin surface vainer mainly for the protection of the crab shell surface. Second and third layers are together called as procuticle. The topmost layer of the procuticle is identified as exocuticle and the bottom layer is referred to as endocuticle. Both these layers mainly consist of calcite crystals which are bound together by a complex matrix of chitin and protein fibers. The striking feature of this fiber matrix is that they show twisted plywood pattern, which is commonly referred to as Bouligand pattern. Individual fiber has a thickness of approximately 60–70 nm which can be further divided to even smaller nanofibers having diameters approximately 3–5 nm (Chen, Lin, McKittrick, & Meyers, 2008; Raabe, Sachs, & Romano, 2005).

Crab shell can be sequentially treated with base, acid and a bleaching agent to remove protein, mineral $CaCO_3$ and colored compounds respectively to obtain chitin. However, during this process chitin is not fibrillated to its primary nanofiber form but rather collapses in to stacks forming chitin flakes. Mechanical processes such as wet grinding and ultrasonication can be used to break inter fiber bonds in these flakes to produce chitin nanofibers (Fan et al., 2012, 2008; Ifuku et al., 2009, 2011; Lu et al., 2013).

Ultrasonication was the method adopted here to disassemble chitin in to nanofibers via cavitation. During the acoustic pressure wave propagation induced by ultrasonication, high and low pressure regions are produced in the medium. At certain instances, the negative pressure can fall below the saturation vapor pressure of the solution at operating temperature resulting a cavity. This cavity can grow, absorbing energy at each cycle until it becomes unstable and finally collapses violently producing shock waves in the medium (Suslick, 1990). Implosions of these cavities can result localized high pressure and high temperature zones that results interactions between particles and shock waves. These extreme environments can encourage processes like fragmentation of matter (Zeiger & Suslick, 2011). Many researches have used the ultrasonication technique to extract nanofibers from natural materials through splitting nanofiber bundles along their axis by breaking weak hydrogen and Van der Waals forces gradually (Cheng, Wang, & Han, 2010; He, Jiang, Zhang, & Pan, 2013; Zhao, Feng, & Gao, 2007). Further ultrasonication of nanofibers can result in scission and fragmentation resulting smaller sizes. These phenomena are observed in carbon nanotubes and some polymer nanofibers (Hennrich et al., 2007; Sawawi, Wang, Nisbet, & Simon, 2013).

Removal of acetyl group from chitin is referred to as deacetylation of chitin. This process can be carried out using a concentrated alkaline solution at high temperature. During deacetylation, nucleophilic attack on carbonyl carbon by hydroxyl ions will result in removal of the acetyl group (Chang, Tsai, Lee, & Fu, 1997). Previous studies on deacetylation of chitin nanowhiskers have shown that the structure and morphology of the whiskers have not significantly change during the process (Antonio, Pereira, & Muniz, 2014; Phongying, Aiba, & Chirachanchai, 2007).

Depolymerization of chitin polymer is known to occur during the deacetylation process due to oxidative degradation of glycoside groups in the polymer chain. The depolymerization is not significant in most cases as the rate of this reaction is lower than that of deacetylation (Chebotok, Novikov, & Konovalova, 2006). However, we could obtain a water soluble component as a byproduct of the process which was confirmed to be chitosan through FTIR analysis. Their solubility at pH values higher than neutral indicates that they are short chain oligomers resulting from depolymerization of chitosan during the reaction.

4.2. AFM characterization

Fig. 2(a) shows the topographical image of chitin nanofibers. Cross sectional analysis of the obtained AFM images revealed that the fiber diameters ranges from 2 to 20 nm with an average diameter around 5 nm. This indicates that complete fibrillation of chitin matrix has occurred during chitin NFs preparation process as fundamental chitin fiber diameter in crab shells falls within this range (Chen et al., 2008; Raabe et al., 2005). The length of majority of nanofibers was in the range of 0.3–4 μm. Nanofiber dimensions were analyzed using vertical height difference to eliminate the inherent error in AFM mapping due to tip convolution effect (Sedin & Rowlen, 2001). Fig. 2(b) shows the topological image of isolated D-chitin NFs after being subjected to ultrasonication for 15 min followed by centrifugation to remove soluble chitosan oligomers. It is possible to identify the presence of both chitosan NPs and chitosan NFs phases as a mixture in this image. Chitosan NFs could be identified as intact structures having higher aspect ratios. Both chitosan NFs and chitosan NPs seem to aggregate during drying resulting an

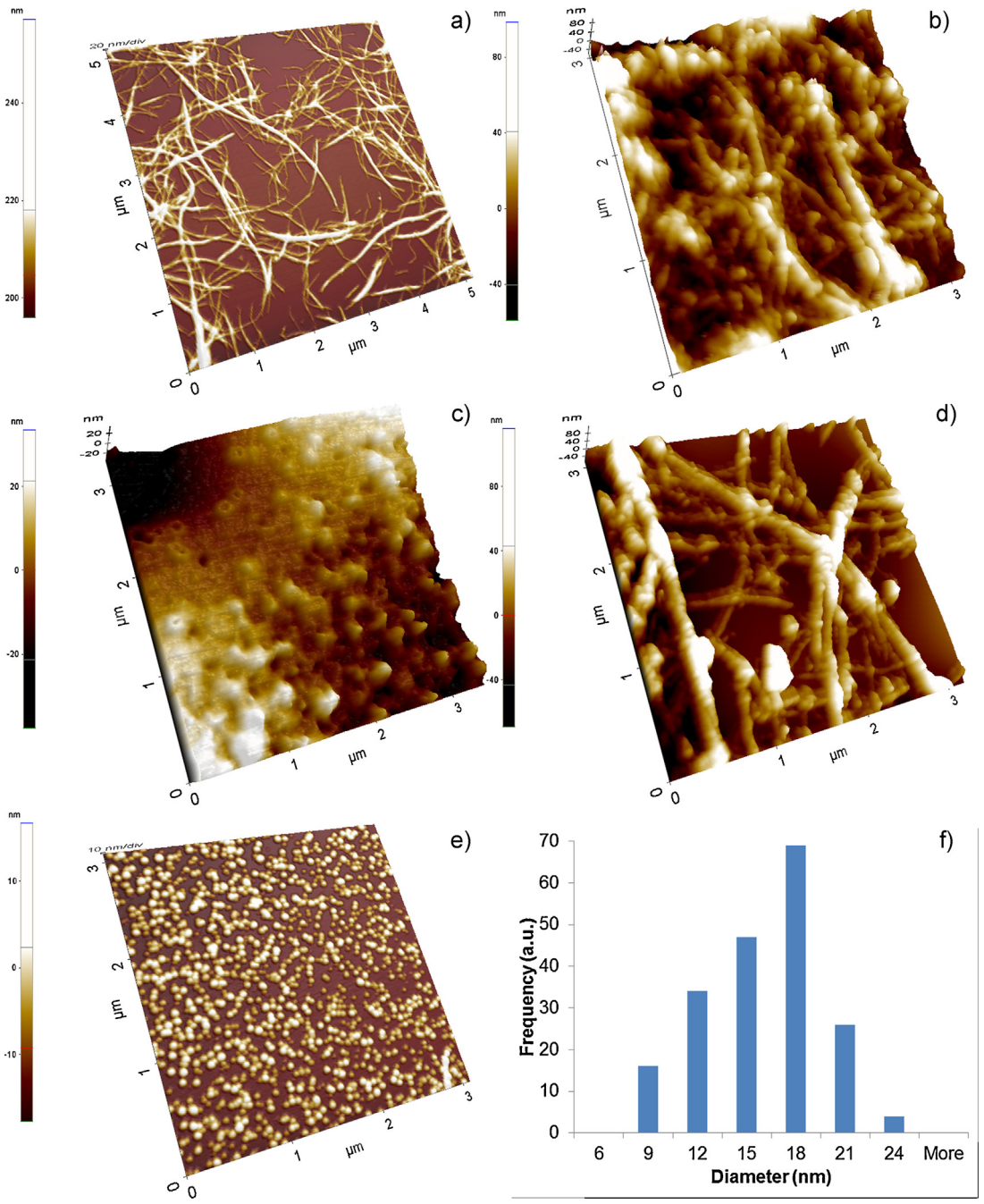

Fig. 2. Topography of (a) chitin nanofibrils, (b) chitosan nanofibers/nanoparticle mixture, (c) casted chitosan oligomer, (d) chitosan nanofibers separated from gravity filtration, (e) chitosan nanoparticles separated from gravity filtration and (f) histogram of chitosan nanoparticle diameter as measured by AFM.

isolated island (not indicated in the figure) which indicates lower electrostatic stability. The water soluble component resulting from deacetylation of chitin NFs is drop casted to observe morphology and shown in Fig. 2(c). It is important to note that solubility of chitosan at pH 6 or higher values typically indicates the presence of low molecular weight chitosan oligomers (Pillai, Paul, & Sharma, 2009; Qin et al., 2006). As expected, the oligomer has no specific shape or regular structure but simulates a topology of a casted polymer film. In contrast, isolated chitosan nanofibers separated by gravity filtration shown in Fig. 2(d) demonstrate a regular fiber mesh like morphology due to the overlaying of large numbers of chitosan NFs. These fibers have high aspect ratios (fiber length divided by fiber diameter) which are typically greater than 50. However, it could also be seen that occasional chitosan nanowhiskers that had lower aspect ratios in the range of 5–30. Topographical image of chitosan NPs separated from gravity filtration is shown in Fig. 2(e). Chitosan NPs could be identified as isolated islands of nanoparticle clusters on the AFM stub indicating lower stability at working pH. Average diameter of nanoparticle as observed by AFM was approximately 15 nm with a diameter range of 9–24 nm as shown in Fig. 2(f).

4.3. TEM characterization

TEM images produced further details on nanomaterial morphologies. As indicated in Fig. 3(a) chitin NFs were seen as large bundles made up of individual nanofibers. These agglomerations were expected during the drying stage on hydrophobic TEM grids due to the fibers with much smaller diameters

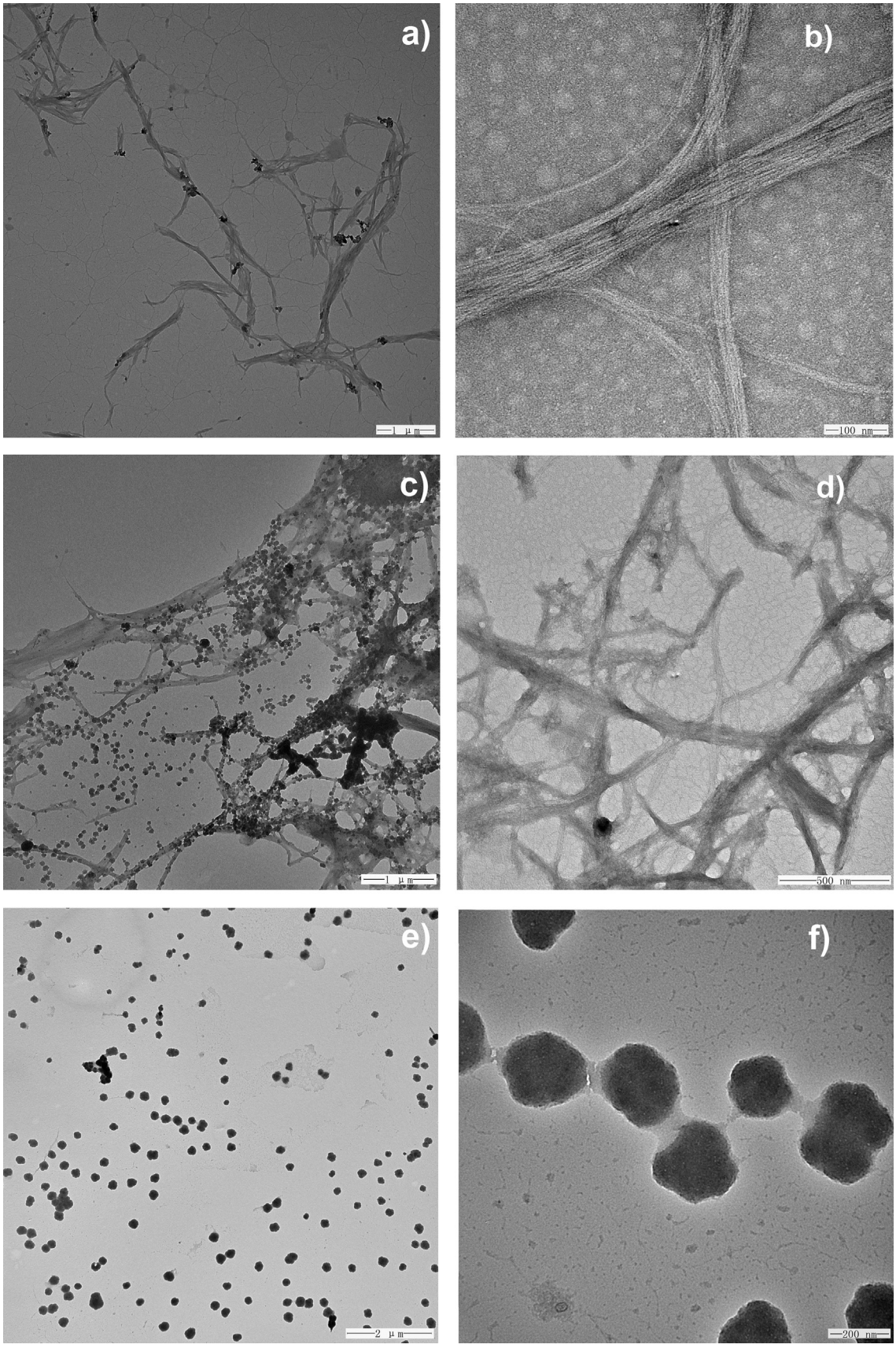

Fig. 3. Tem images of (a) chitin NFs, (b) chitin NFs in higher magnification, (c) chitosan NPs and chitosan NFs mixture, (d) chitosan NFs, (e) chitosan NPs and (f) higher magnification image of chitosan NPs.

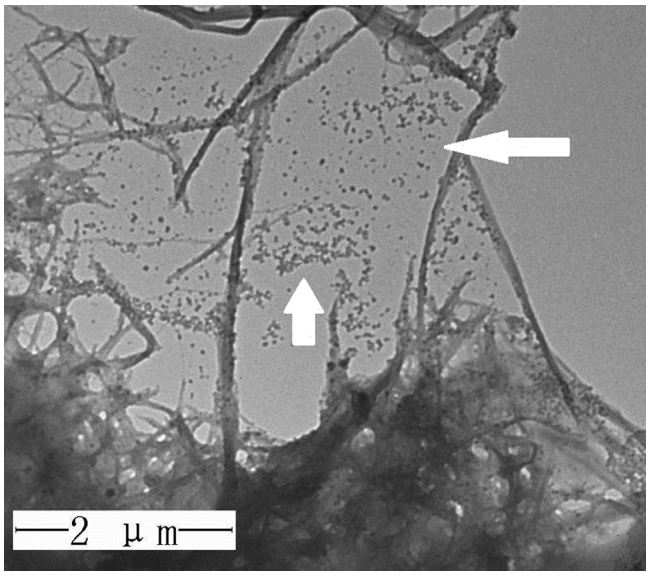

Fig. 4. Nanoparticles having less than 30 nm diameter found in chitosan NPs and chitosan NFs mixture.

were observed around the large bundles. Occasional debris was also observed, possibly formed during the chitin NFs preparation process. Fig. 3(b) shows a magnified image of isolated chitin NFs. Close inspection of the TEM images shows that the fiber diameter is less than 10 nm. Observed nanofiber lengths ranged from 0.5 to 4 μm which in agreement with AFM analysis.

Fig. 3(c) shows the morphology of chitosan NPs and chitosan NFs mixture. It could clearly be seen that both nanofiber and nanoparticle phases are present in the mixture. Close analysis revealed that large bundles seen in the TEM images are due to the blend of smaller nanofibers. Chitosan NPs were adhered to chitosan NFs, resulting an aggregated structure.

TEM image of chitosan NFs is shown in Fig. 4(d). Majority of the fibers have diameters less than 100 nm and lengths less than 3 μm. It is possible that during the process of deacetylation alkali has penetrated the chitin NFs structure resulting a swollen fiber. We could also observe small nanofiber aggregates to make larger nanofiber bundles. When compared with chitin NFs, chitosan NFs appears to be less defined in the TEM images indicating the amorphous structure of these nanofibers. Also, nanofiber bundles were made out of much shorter nanofibers than in the case of chitin NFs. This is possibly due to the lengthwise scissoring of these small nanofibers due to cavitation in the preparation process.

Nanoparticles which have irregular shapes were scattered on the surface. The Observed diameters of nanoparticles were less than 300 nm (Fig. 3(e)). This presents a contradiction between the AFM and TEM data on chitosan NPs diameter as AFM suggested that the diameters of nanoparticle are less than 25 nm. However, this discrepancy could be explained by careful analysis of the TEM images. In certain locations isolated patches of chitosan NPs due to much smaller diameters (less than 30 nm) could be observed (Fig. 4). We could expect that these nanoparticles act as building blocks for large nanoparticles that were frequently observed in the sample. Single nanoparticles could be identified as composed of a number of smaller nanoparticles which are produced during sonication of chitosan nanofibers (Fig. 3(f)).

4.4. FTIR characterization

The FTIR spectra of chitin flakes, chitin NFs and chitosan NPs and chitosan NFs mixture are shown in Fig. 5. FTIR spectra for chitin flakes and chitin NFs are in accordance with the previously published work (Cárdenas, Cabrera, Taboada, & Miranda, 2004; Ifuku et al., 2009, 2011). The broad and weak absorption bands from 3600 cm^{-1} to 3000 cm^{-1} are due to the combined absorption by N—H and O—H groups in the chitin polymer (Fig. 5(a) and (b)). The absorption band at 3253 cm^{-1} in chitin flakes and 3458 cm^{-1} in chitin NFs can be attributed to the N—H secondary amine stretch. The absorption band due to the presence of NH—CO group in the chitin structure is located at 3101 cm^{-1}. The weak absorption band in the region of 2961–2829 cm^{-1} is due to the presence of methylene and methyl groups in the chitin structure and originates due to the C—H bond of sp^3 hybridized carbon. The spectra also show the presence of two bands in the region of 1660–1620 cm^{-1}. Both these bands are due to the C=O stretching vibration of the amide I bonds. Splitting of the peak in to two characteristic bands at 1655 cm^{-1} and ~1620 cm^{-1} is due to the influence of hydrogen bonding in the polymeric structure. The absorption peak at ~1553 cm^{-1} is due to the presence of N—H of Amide II bond structure in the polymer. Bond absorptions in the region of 1420–700 cm^{-1} are due to a number of chemical functionalities in the pyranose ring including —CHx, —C—O—C— and —OH.

The FTIR spectrum for chitosan NPs and chitosan NFs mixture is shown in Fig. 5(c). The spectrum is similar to chitin vibration patterns but with significant changes in the positions and intensities. The broad absorption band which appear in the range of 3600–2800 cm^{-1} can be related to collective absorption by both N—H and O—H groups in the polymer. The broad absorption is a good indication for the strong hydrogen bonded intermolecular structure. The absorption peak at ~1553 cm^{-1} in chitin has disappeared and two new peaks have emerged at 1652 cm^{-1} and 1597 cm^{-1} indicating successful deacetylation. The peak which appears at 1652 cm^{-1} can be assigned to amide I absorption and peak at 1597 cm^{-1} is due to the amide II functionality in the chitosan polymer. The degree of deacetylation of the sample was evaluated by the method proposed by Baxter, Dillon, Anthony Taylor, and Roberts (1992). Absorption ratio between peaks at 1652 cm^{-1} (amide I) and 3450 cm^{-1} is used to calculate the percent degree of deacetylation as follows:

$$\%\,\text{Degree of deacetylation} = 100 - \frac{A_{1652}}{A_{3450}} \times 115 \quad (1)$$

From this the degree of deacetylation for chitosan NPs and chitosan NFs mixture is approximately 98%.

4.5. XRD characterization

XRD spectra of chitin flakes, chitin NFs and chitosan NPs and chitosan NFs mixture are shown in Fig. 6. For chitin flakes and chitin NFs, four major diffraction peaks were identified and they are located around 9.5°, 19.5°, 20.9°, and 23.4°. These peaks correspond to the 0 2 0, 1 1 0, 1 2 0, 1 3 0 crystal planes respectively, and are typical crystal patterns of α-chitin (Maniukiewicz, 2011; Zhang, Xue, Xue, Gao, & Zhang, 2005). Peaks closely coincide with each other indicating that the crystal structure has been maintained even after the chemical and mechanical treatment. Chitosan on the other hand shows broad diffraction peaks indicating amorphous polymer structure compared to chitin. This can be due to the significant distortion of macromolecular configuration induced by strong deacetylation conditions. Two main diffraction peaks were identified and are located at 10–11° and at 20–21°.

4.6. Thermogravimetric analysis

Results from thermogravimetric analyses carried out under N_2 environment for chitin flakes, chitin NFs, chitosan flakes and chitosan NPs and chitosan NFs mixture are shown in Fig. 7. All the

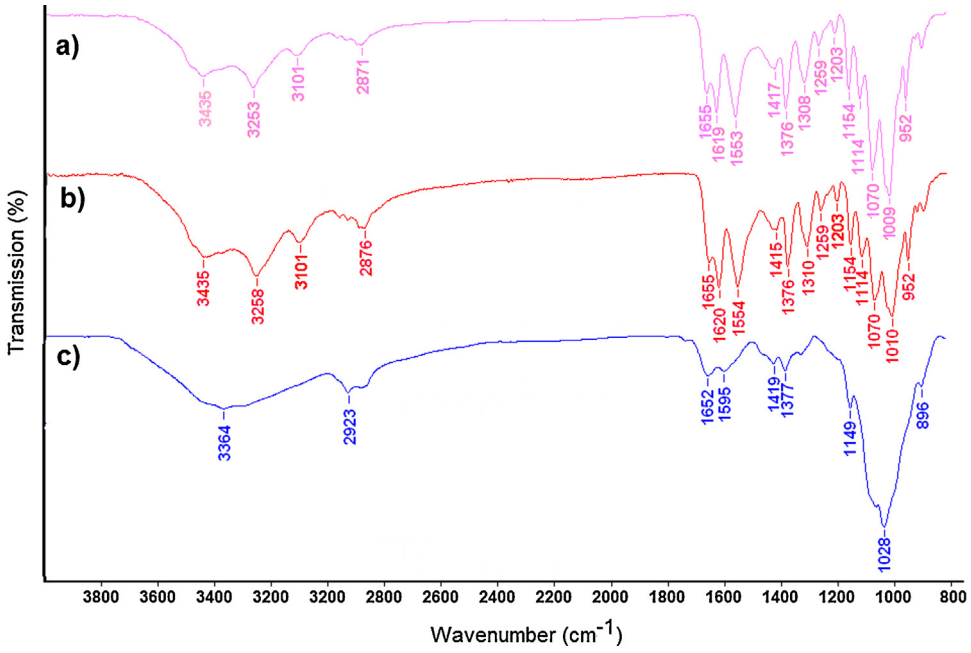

Fig. 5. FT-IR spectra of (a) chitin flakes, (b) chitin NFs and (c) chitosan NPs and chitosan NFs mixture.

samples show a slight decrease of weight bellow 100 °C indicating loss of absorbed moisture. From all the samples, chitin flakes had the highest degradation temperature (T_d) around 403 °C at highest degradation rate which indicate strong hydrogen bonded chemical structure. As shown in Fig. 7(b) the degradation rate of chitin flake is higher as compared to others. This indicates relatively undisturbed packing of chitin polymers in the structure. However, chitin NFs show slightly low T_d of 338 °C at the highest degradation rate. This suggests that the hydrogen bonding structure of chitin NFs is further disturbed possibly due to the chemical and mechanical treatments employed during the preparation process. Rate of degradation of chitin NFs is lower than that of chitin flakes. In contrast to the chitin flakes and chitin NFs, chitosan flakes and chitosan NPs and chitosan NFs mixture does not show significant difference in T_d values and ash contents. TGA results are similar to reports published previously (Phongying et al., 2007).

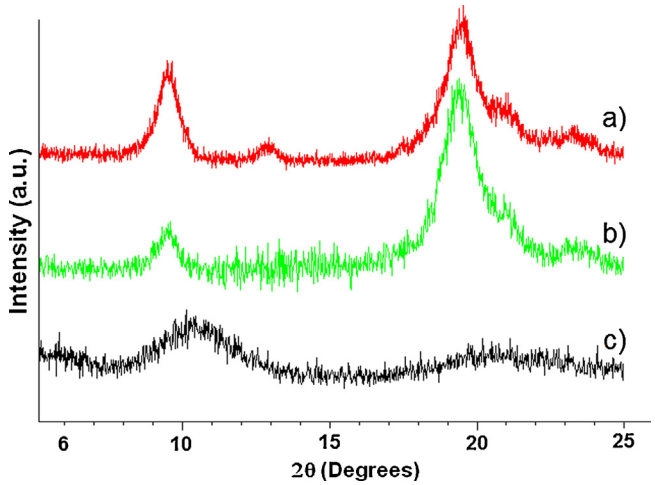

Fig. 6. XRD spectrum of (a) chitin flakes, (b) chitin NFs and (c) chitosan NPs and chitosan NFs mixture.

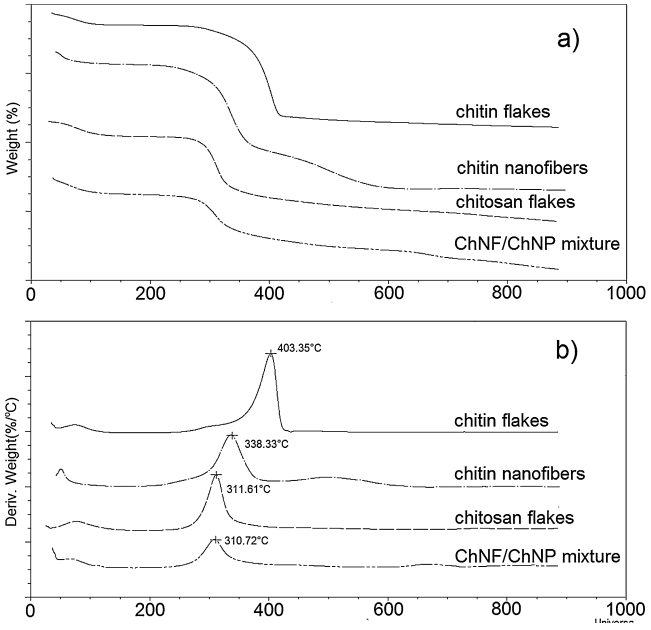

Fig. 7. TGA thermograms showing (a) weight percentage of different systems and (b) derivative weight percentage with respect to temperature.

5. Conclusion

This paper reports a top down preparation method of chitosan nanoparticles and chitosan nanofibers employing direct ultrasonication of deacetylated chitin nanofibers. Pure chitin isolated from crab shells was treated chemically and mechanically to obtain chitin nanofibers. These nanofibers were then deacetylated under alkaline conditions followed by ultrasonic treatment. This process leads to chitin nanofibers were having diameters less than 20 nm and lengths less than 4 μm. Ultrasonication of deacetylated chitin nanofibers resulted in a mixture of chitosan nanoparticles and nanofibers. Chitosan nanoparticles could be isolated using simple

gravity filtration and had diameters less than 300 nm. However, these nanoparticles were observed to be made out of much smaller nanoparticles which had diameters less than 25 nm. The prepared chitosan has a degree of deacetylation close to 98% and amorphous in structure. We show that chitosan nanoparticles and nanofibers can be made using direct ultrasonication of deacetylated chitin nanofibers.

Acknowledgement

We would like to thank Prof. Qian Wang, Department of Chemistry, University of South Carolina, USA for help in material characterization.

References

Andersen, O., Hägerstrand, I., & Nordberg, G. F. (1982). Effect of the chelating agent sodium tripolyphosphate on cadmium toxicity in mice. *Environmental Research*, *29*(1), 54–61.

Antonio, G. B., Pereira, E. C., & Muniz, Y.-L. H. (2014). Chitosan-sheath and chitin-core nanowhiskers. *Carbohydrate Polymers*, *107*, 158–166.

Baxter, A., Dillon, M., Anthony Taylor, K. D., & Roberts, G. A. F. (1992). Improved method for i.r. determination of the degree of N-acetylation of chitosan. *International Journal of Biological Macromolecules*, *14*(3), 166–169.

Cárdenas, G., Cabrera, G., Taboada, E., & Miranda, S. P. (2004). Chitin characterization by SEM, FTIR, XRD, and 13C cross polarization/mass angle spinning NMR. *Journal of Applied Polymer Science*, *93*(4), 1876–1885.

Chang, K. L. B., Tsai, G., Lee, J., & Fu, W.-R. (1997). Heterogeneous N-deacetylation of chitin in alkaline solution. *Carbohydrate Research*, *303*(3), 327–332.

Chebotok, E. N., Novikov, V. Y., & Konovalova, I. N. (2006). Depolymerization of chitin and chitosan in the course of base deacetylation. *Russian Journal of Applied Chemistry*, *79*(7), 1162–1166.

Chen, P.-Y., Lin, A. Y.-M., McKittrick, J., & Meyers, M. A. (2008). Structure and mechanical properties of crab exoskeletons. *Acta Biomaterialia*, *4*(3), 587–596.

Cheng, Q., Wang, S., & Han, Q. (2010). Novel process for isolating fibrils from cellulose fibers by high-intensity ultrasonication. II. Fibril characterization. *Journal of Applied Polymer Science*, *115*(5), 2756–2762.

Elsabee, M. Z., Naguib, H. F., & Morsi, R. E. (2012). Chitosan based nanofibers, review. *Materials Science and Engineering: C*, *32*(7), 1711–1726.

Fan, Y., Fukuzumi, H., Saito, T., & Isogai, A. (2012). Comparative characterization of aqueous dispersions and cast films of different chitin nanowhiskers/nanofibers. *International Journal of Biological Macromolecules*, *50*(1), 69–76.

Fan, Y., Saito, T., & Isogai, A. (2008). Preparation of chitin nanofibers from Squid Pen β-chitin by simple mechanical treatment under acid conditions. *Biomacromolecules*, *9*(7), 1919–1923.

Fan, Y., Saito, T., & Isogai, A. (2010). Individual chitin nano-whiskers prepared from partially deacetylated alpha-chitin by fibril surface cationization. *Carbohydrate Polymers*, *79*(4), 1046–1051.

Fuente, M. d. l., Raviña, M., Paolicelli, P., Sanchez, A., Seijo, B., & Alonso, M. J. (2010). Chitosan-based nanostructures: A delivery platform for ocular therapeutics. *Advanced Drug Delivery Reviews*, *62*(1), 100–117.

Garcia-Fuentes, M., & Alonso, M. J. (2012). Chitosan-based drug nanocarriers: Where do we stand? *Journal of Controlled Release*, *161*(2), 496–504.

Grenha, A. (2012). Chitosan nanoparticles: A survey of preparation methods. *Journal of Drug Targeting*, *20*(4), 291–300.

He, W., Jiang, S., Zhang, Q., & Pan, M. (2013). Isolation and characterization of cellulose nanofibers from *Bambusa rigida*. *BioResources*, *8*(4).

Hennrich, F., Krupke, R., Arnold, K., Rojas Stiiz, J. A., Lebedkin, S., Koch, T., et al. (2007). The mechanism of cavitation-induced scission of single-walled carbon nanotubes. *The Journal of Physical Chemistry B*, *111*(8), 1932–1937.

Ifuku, S., Nogi, M., Abe, K., Yoshioka, M., Morimoto, M., Saimoto, H., et al. (2009). Preparation of chitin nanofibers with a uniform width as alpha-chitin from crab shells. *Biomacromolecules*, *10*(6), 1584–1588.

Ifuku, S., Nogi, M., Abe, K., Yoshioka, M., Morimoto, M., Saimoto, H., et al. (2011). Simple preparation method of chitin nanofibers with a uniform width of 10–20 nm from prawn shell under neutral conditions. *Carbohydrate Polymers*, *84*(2), 762–764.

Iqbal, P., Preece, J. A., & Mendes, P. M. (2012). Nanotechnology: The top-down and bottom-up approaches. In J. W. Steed, & P. A. Gale (Eds.), *Supramolecular chemistry*. Oxford: John Wiley & Sons, Ltd.

Jayakumar, R., Prabaharan, M., Nair, S. V., & Tamura, H. (2010). Novel chitin and chitosan nanofibers in biomedical applications. *Biotechnology Advances*, *28*(1), 142–150.

Jayakumar, R., Prabaharan, M., Sudheesh Kumar, P. T., Nair, S. V., & Tamura, H. (2011). Biomaterials based on chitin and chitosan in wound dressing applications. *Biotechnology Advances*, *29*(3), 322–337.

Liu, D., Chang, P. R., Chen, M., & Wu, Q. (2011). Chitosan colloidal suspension composed of mechanically disassembled nanofibers. *Journal of Colloid and Interface Science*, *354*(2), 637–643.

Liu, D., Wu, Q., Chang, P. R., & Gao, G. (2011). Self-assembled liquid crystal film from mechanically defibrillated chitosan nanofibers. *Carbohydrate Polymers*, *84*(1), 686–689.

Lu, Y., Sun, Q., She, X., Xia, Y., Liu, Y., Li, J., et al. (2013). Fabrication and characterisation of α-chitin nanofibers and highly transparent chitin films by pulsed ultrasonication. *Carbohydrate Polymers*, *98*(2), 1497–1504.

Maniukiewicz, W. (2011). X-ray diffraction studies of chitin, chitosan and their derivatives. In S.-K. Kim (Ed.), *Chitin, chitosan, oligosaccharides and their derivatives* (Vol. 1). Boca Raton, FL: CRC Press Print.

Muzzarelli, R. A. A. (2011). Biomedical exploitation of chitin and chitosan via mechano-chemical disassembly, electrospinning, dissolution in imidazolium ionic liquids, and supercritical drying. *Marine Drugs*, *9*(9), 1510–1533.

Muzzarelli, R. A. A. (2012). Nanochitins and nanochitosans, paving the way to eco-friendly and energy-saving exploitation of marine resources. *Polymer Science: A Comprehensive Reference*, *10*, 153–164.

Phongying, S., Aiba, S.-i., & Chirachanchai, S. (2007). Direct chitosan nanoscaffold formation via chitin whiskers. *Polymer*, *48*(1), 393–400.

Pillai, C. K. S., Paul, W., & Sharma, C. P. (2009). Chitin and chitosan polymers: Chemistry, solubility and fiber formation. *Progress in Polymer Science*, *34*(7), 641–678.

Qin, C., Li, H., Xiao, Q., Liu, Y., Zhu, J., & Du, Y. (2006). Water-solubility of chitosan and its antimicrobial activity. *Carbohydrate Polymers*, *63*(3), 367–374.

Raabe, D., Sachs, C., & Romano, P. (2005). The crustacean exoskeleton as an example of a structurally and mechanically graded biological nanocomposite material. *Acta Materialia*, *53*(15), 4281–4292.

Sawawi, M., Wang, T. Y., Nisbet, D. R., & Simon, G. P. (2013). Scission of electrospun polymer fibres by ultrasonication. *Polymer*, *54*(16), 4237–4252.

Sedin, D. L., & Rowlen, K. L. (2001). Influence of tip size on AFM roughness measurements. *Applied Surface Science*, *182*(1–2), 40–48.

Shukla, S. K., Mishra, A. K., Arotiba, O. A., & Mamba, B. B. (2013). Chitosan-based nanomaterials: A state-of-the-art review. *International Journal of Biological Macromolecules*, *59*(0), 46–58.

Suslick, K. S. (1990). Sonochemistry. *Science*, *247*(4949), 1439–1445.

Zeiger, B. W., & Suslick, K. S. (2011). Sonofragmentation of molecular crystals. *Journal of the American Chemical Society*, *133*(37), 14530–14533.

Zeiger, E., Gollapudi, B., & Spencer, P. (2005). Genetic toxicity and carcinogenicity studies of glutaraldehyde – A review. *Mutation Research/Reviews in Mutation Research*, *589*(2), 136–151.

Zhang, Y., Xue, C., Xue, Y., Gao, R., & Zhang, X. (2005). Determination of the degree of deacetylation of chitin and chitosan by X-ray powder diffraction. *Carbohydrate Research*, *340*(11), 1914–1917.

Zhao, H.-P., Feng, X.-Q., & Gao, H. (2007). Ultrasonic technique for extracting nanofibers from nature materials. *Applied Physics Letters*, *90*(7), 073112.

Zhong, C., Cooper, A., Kapetanovic, A., Fang, Z., Zhang, M., & Rolandi, M. (2010). A facile bottom-up route to self-assembled biogenic chitin nanofibers. *Soft Matter*, *6*(21), 5298–5301.

Zhou, C., & Wu, Q. (2011). A novel polyacrylamide nanocomposite hydrogel reinforced with natural chitosan nanofibers. *Colloids and Surfaces B: Biointerfaces*, *84*(1), 155–162.